Quantitative Analysis of Phospholipids in Functionally Important Membrane Domains from RBL-2H3 Mast Cells Using Tandem High-Resolution Mass Spectrometry†

Einar K. Fridriksson,‡ Petia A. Shipkova,‡,§ Erin D. Sheets, David Holowka,* Barbara Baird,* and Fred W. McLafferty*

Department of Chemistry and Chemical Biology, Baker Laboratory, Cornell University, Ithaca, New York 14853-1301

Received December 2, 1998; Revised Manuscript Received April 15, 1999

ABSTRACT: We recently showed that ligand-mediated cross-linking of FcεRI, the high-affinity receptor for immunoglobulin E, on RBL-2H3 mast cells results in its co-isolation with detergent-resistant membranes (DRM) and its consequent tyrosine phosphorylation by the co-localized tyrosine kinase Lyn that is a critical early event in signaling by this receptor [Field et al. (1997) *J. Biol. Chem. 272*, 4276−4280]. As part of efforts to determine the structural bases for these interactions, we examined the phospholipid composition of DRM vesicles isolated from RBL-2H3 cells under conditions that preserve FcεRI association. We used positive and negative mode electrospray Fourier transform ion cyclotron resonance mass spectrometry to compare quantitatively the phospholipid composition of isolated DRM to that of total cell lipids and to a plasma membrane preparation. From these analyses, over 90 different phospholipid species were spectrally resolved and unambiguously identified; more than two-thirds of these were determined with a precision of ±0.5% (absolute) or less. Quantitative characterization of lipid profiles shows that isolated DRM are substantially enriched in sphingomyelin and in glycerophospholipids with a higher degree of saturation as compared to total cellular lipids. Plasma membrane vesicles isolated from RBL-2H3 cells by chemically induced blebbing exhibit a degree of phospholipid saturation that is intermediate between DRM and total cellular lipids, and significant differences in the headgroup distribution between DRM and plasma membranes vesicles are observed. DRM from cells with cross-linked FcεRI exhibit a larger ratio of polyunsaturated to saturated and monounsaturated phospholipids than those from unstimulated cells. Our results support and strengthen results from previous studies suggesting that DRM have a lipid composition that promotes liquid-ordered structure. Furthermore, they demonstrate the potential of mass spectrometry for examining the role of membrane structure in receptor signaling and other cellular processes.

There is increasing interest in the existence and possible functional roles for specialized regions in the plasma membrane of eukaryotic cells (*1*). Recent studies have identified candidate membrane domains [variously called DRM,[1] DIG (detergent-insoluble glycolipid domains), GEM (glycolipid-enriched membranes), and lipid rafts] based on the resistance of certain plasma membrane components to solubilization into mixed micelles by the non-ionic detergent Triton X-100 (*2, 3*). In particular, certain lipid-anchored proteins, sphingolipids, and cholesterol are enriched in DRM vesicles that can be isolated by flotation in sucrose density gradients. The acyl chains of these lipid-anchored proteins and sphingolipids are known to be largely saturated, and Brown and colleagues showed that model membranes comprising these same types of components, together with cholesterol, have the same properties of detergent resistance and buoyancy (*4*). Furthermore, they showed with fluorescence probes that model membranes of this composition have a liquid-ordered (L_o) structure in which the lipids are fluid, similar to the liquid crystalline phase, but their acyl chains exhibit a high degree of lateral ordering, similar to the gel phase (*5, 6*). Other physical measurements also reveal a L_o structure in model membranes containing phospholipids with saturated acyl chains and cholesterol as major components (*7*−*10*).

We recently provided evidence for the functional importance of DRM as regions for coupling between FcεRI and Lyn, a Src family tyrosine kinase, on RBL-2H3 mast cells (*11, 12*). The Lyn protein is anchored to the inner leaflet of the plasma membrane bilayer by means of dual acylation at its N-terminus with myristate and palmitate (*13, 14*), and it co-isolates with DRM components following Triton X-100 lysis of RBL-2H3 cells and sucrose gradient ultracentifugation (*15*). Cross-linking of IgE−FcεRI complexes by multivalent ligands on cells initiates signaling by this receptor

† Supported by National Institutes of Health Grants GM 16609, AI 18306, and AI 09838 (E.D.S.).

‡ These authors contributed equally to this study.

§ Present address: Schering-Plough Research Institute, 2015 Galloping Hill Rd., K-15-1945, Kenilworth, NJ 07033.

[1] Abbreviations: CAD, collisionally activated dissociation; DRM, detergent-resistant membranes; ESI, electrospray ionization; FTMS, Fourier transform mass spectrometry; MS/MS, tandem mass spectrometry; PA, phosphatidic acid; PC, phosphatidylcholine; PE, phosphatidylethanolamine; PG, phosphatidylglycerol; PI, phosphatidylinositol; PS, phosphatidylserine; SM, sphingomyelin; SWIFT, stored waveform inverse Fourier transform; TLE, total lipid extract.

10.1021/bi9828324 CCC: $18.00
Published on Web 05/28/1999

and causes its association with gradient-isolated DRM vesicles, but only if the detergent concentration is reduced 10-fold compared to standard lysis conditions (*11*). Under these same conditions of low detergent, un-cross-linked IgE−FcεRI are solubilized and thus do not co-isolate with the DRM, pointing to a functionally relevant correlation between receptor cross-linking and DRM association. Furthermore, the receptors that are tyrosine phosphorylated in intact cells co-isolate with DRM after lysis, suggesting that this membranous interaction is important for signal initiation in vivo. Efficient in vitro tyrosine phosphorylation of FcεRI co-isolated with DRM provides evidence that these isolated membrane structures are also conducive to efficient Lyn−FcεRI coupling (*11*). We recently found that cholesterol is critical for this receptor phosphorylation on intact cells as well as for the interactions of Lyn and cross-linked FcεRI with isolated DRM (*16*). However, other features of DRM and FcεRI that are important for these interactions are not well understood.

It is likely that selective lipid−lipid and lipid−protein interactions are primary determinants of DRM structure, including cross-link-dependent association of FcεRI with these structures. For essential insight, it is thus important to determine the detailed lipid composition of DRM and to investigate any changes in lipid composition that may accompany FcεRI cross-linking and signal initiation. Mass spectrometry is an accurate and sensitive analytical technique for lipid detection, identification, and quantification (*17*−*22*). Compared to other techniques commonly used for analysis of complex lipid mixtures such as thin-layer chromatography (TLC), tandem mass spectrometry (MS/MS) (*18*, *19*, *23*) is clearly superior in sensitivity and resolution. For MS/MS, a soft ionization, such as electrospray ionization (ESI) (*24*), produces molecular ions for each mixture component. Ions of a specific mass/charge (*m*/*z*) value, separated in the first dimension (MS-I), are dissociated to produce a second-dimension spectrum (MS-II) characteristic of the isomeric structure. Fourier transform mass spectrometry (FTMS) provides the special advantage of high ($\sim 10^5$) resolving power (*25*) in both MS-I and MS-II, which allows identification of many different lipid components in a single sample. Using this information, we have been able to quantify and compare the complex phospholipid compositions of isolated DRM, plasma membrane vesicles, and total cellular lipids.

MATERIALS AND METHODS

Preparation of Total Lipid Extracts (TLE). RBL-2H3 cells ($5-10 \times 10^7$) were harvested in 1.5 mM EDTA/saline, pelleted by centrifugation (200*g*, 8 min), and washed twice in buffered saline solution (BSS: 135 mM NaCl, 5 mM KCl, 1 mM $MgCl_2$, 1.8 mM $CaCl_2$, 5.6 mM glucose, 20 mM HEPES, pH 7.4, 1 mg/mL BSA) as previously described (*26*). After the second wash, the cells were resuspended in 5 mL of distilled, deionized water, then centrifuged again, resuspended in 5 mL of methanol, and transferred to a Duall ground glass tissue grinder. After 20 strokes, 5 mL of chloroform was added, and the suspension was probe-sonicated (Vibra Cell ASI, Sonics & Materials, Danbury, CT) at highest power for 5 min at 45 °C and then rocked for at least 2 h at room temperature. This suspension was centrifuged for 10 min at 400*g*, and the supernatant was collected. The pellet was re-extracted in 5 mL of 1:1 chloroform:methanol (v/v) and centrifuged again. The collected supernatants were pooled and lyophilized.

The lyophilized residue was resuspended in 0.6 mL of 60:40 v/v diisopropyl ether:1-butanol, vortexed, and bath-sonicated for 10−15 min, followed by addition of 0.3 mL of 50 mM NaCl and a second round of vortexing and sonication (*27*). The mixture was centrifuged at 200*g* for 10 min, and the upper (organic) phase was collected. The lower (aqueous) phase was re-extracted with 0.3 mL of diisopropyl ether:1-butanol, and the upper phases were combined and lyophilized. The resulting lipid film was dissolved in 250 μL of 1:1 methanol:chloroform (v/v) and analyzed by mass spectrometry as described below.

DRM Vesicle Isolation. RBL-2H3 cells were harvested as described above and resuspended in BSS at a density of 8×10^6 cells/mL. For some experiments, cells were sensitized with 1 μg/mL biotinylated IgE (*15*) at least 4 h prior to harvesting. For cross-linking of biotinylated IgE−FcεRI complexes, 10 nM streptavidin was added and the cells were incubated at 37 °C for 5 min just prior to cell lysis. Cells in BSS (typically 15 mL of 8×10^6 cells/mL in each sample) were lysed by mixing 1:1 with 2× ice-cold lysis buffer containing 0.08−0.1% Triton X-100 (v/v) as previously described (*11*). The cell lysates were then diluted with an equal volume of 80% sucrose (w/v) in HEPES/saline buffer (25 mM HEPES, 150 mM NaCl, 2 mM EDTA, pH 7.5) at 4 °C; 20 mL of this lysate was added to each polycarbonate centrifuge tube (Beckman Corp., Palo Alto, CA), and then 5 mL of 35% sucrose and 5 mL of 5% sucrose solutions in buffer were sequentially layered on the top of the 40% sucrose lysate. These tubes were centrifuged in a Beckman SW28 rotor at 100000*g* for 12−18 h at 4 °C in a Beckman L8-70M ultracentrifuge. After centrifugation, two opaque bands were visible near the top of the centrifuge tubes. The upper band was located at the interface between the 5% and 35% sucrose layers and contained the DRM as determined by co-migration of [^{125}I]IgE bound to FcεRI under cross-linking conditions (*11*) and by the co-migration of [^{125}I]AA4 mAb bound to α-galactosyl GD_{1b} ganglioside derivatives (*15*). The upper band material was collected, diluted 2−3-fold in 40 mM HEPES, pH 7.4, and centrifuged at 300000*g* in a Beckman Ti60 rotor for 1 h at 10 °C. The pelleted DRM vesicles were resuspended in 25 mL of the HEPES buffer and centrifuged. The pellet was then subjected to lipid extraction as described above for intact cells, starting with 1 mL of methanol/$8-12 \times 10^7$ cell equiv of DRM.

Plasma Membrane Vesicle Isolation. Plasma membrane vesicles were isolated from RBL-2H3 cells following chemical induction of "cell blebbing" as previously described (*28*). This preparation was shown to be free of contamination from intracellular membranes and representative of plasma membranes as previously described (*29*). Other experiments showed that blebs still attached to cells contain laterally mobile components, but not cytoskeletally associated immobile components (*30*), suggesting that the plasma membrane vesicles isolated by blebbing contain representative composition of mobile plasma membrane proteins and lipids.

Mass Spectrometry Analysis. All samples were nanosprayed as previously described (*31*, *32*) from 49:49:2 (v/v) methanol:chloroform:acetic acid for the positive ion mode and from 50:50 (v/v) methanol:chloroform for the negative

Chart 1

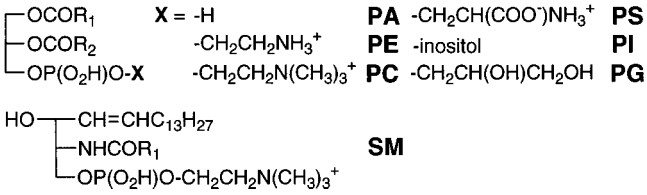

ion mode. Typically, less than 2×10^5 cell equiv of the lipid extract [<6 nmol of phospholipid (*33*)] are needed to obtain a complete spectrum. The modified 6T Finnigan (Madison, WI) FTMS instrument is described in detail elsewhere (*34*). For MS/MS experiments the ions of interest were isolated in the cell chamber using stored waveform inverse Fourier transform (SWIFT) (*35*) and further subjected to collisionally activated dissociation (CAD) (*36*−*38*) which produces fragment ions specific for each parent ion. Phospholipid standards for phosphatidic acid (PA), phosphatidylcholine (PC), phosphatidylethanolamine (PE), phosphatidylglycerol (PG), phosphatidylserine (PS), and phosphatidylinositol (PI) were obtained from Avanti Polar Lipids (Alabaster, AL); PI was purified from bovine liver, and others were synthetic dioleyl phospholipids. Sphingomyelin (SM; purified from bovine brain) was obtained from Matreya (Pleasant Gap, PA).

To determine the phospholipid compositions of the lipid extracts, the relative sensitivities of detection of different phospholipid classes were determined using a 1.00:0.98:1.42 molar mixture (1:1:1.5 w/v) of PE:PC:SM standards for the positive ion mode and a 1.00:1.06:0.96:0.94:0.85 molar mixture (1:1:1:1:1 w/v) of PE:PA:PG:PS:PI standards for the negative ion mode. The relative intensity of PE in positive and negative ion modes was used to normalize these spectra with respect to each other. For this comparison, 0.3% NH_4OH (v/v) was added to the negative ion standard mixture to ensure deprotonation; this addition was found to have no significant effect on the negative ion spectra for the RBL-2H3 membrane lipid samples.

RESULTS

Biological membranes contain a large number of different phospholipid molecules, most of which belong to one of the seven major classes as shown in Chart 1. These different phospholipid molecules can be detected and quantified in a complex mixture using mass spectrometry. When subjected to CAD, positive and negative ions generated in ESI of the phospholipids PC, PE, PS, and SM lose their polar headgroups, and PI and PG lose their acyl chains (*18*, *19*). This selective fragmentation gives sufficient information to identify each phospholipid type in a complex mixture. Figure 1 illustrates the assignment process for the major peaks at *m*/*z* 808.6 and 809.6 from a positive ion spectrum of RBL-2H3 cell TLE. These correspond to $^{12}C_{46}H_{83}NO_8P$ and $^{12}C_{45}{}^{13}C_1H_{83}NO_8P$, reflecting the 1.1% natural abundance of ^{13}C and also show that these ions are singly charged ($z = 1$). These ions were isolated by SWIFT, and their fragmentation by CAD caused the loss of 183 mass units corresponding to a phosphoryl choline headgroup; the appearance of a new peak at mass 625.5 corresponds to a glycerol backbone with two acyl chains containing a total of 38 carbon atoms (including the two CO groups) and 5 double bonds (38:5). This assignment is consistent, for example, with a PC

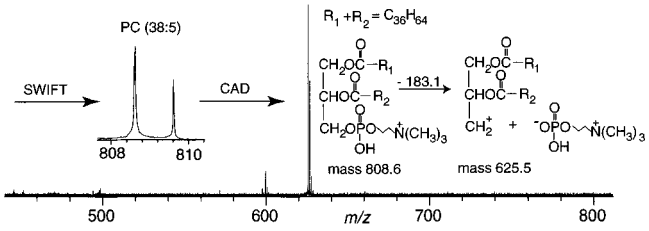

FIGURE 1: MS/MS spectrum of a parent ion at 808.6 Da (insert, left) shows a fragment at 625.5 Da. The 183 Da mass difference between the parent and product ion corresponds to a phosphatidyl phosphoryl choline headgroup, as shown. The 1.1% natural abundance of ^{13}C produces the peaks of ~50% abundance 1 Da larger than the major peaks.

molecule containing oleyl (18:1) and arachidonyl (20:4) fatty acid chains; however, only the total numbers of acyl chain carbons and double bonds are determined and reported here. PC and SM have the same polar headgroups, and thus both of these phospholipids lose a fragment of mass 183. However, SM has two nitrogen atoms in its structure, whereas PC has only one, resulting in odd and even mass units, respectively, thus distinguishing the two species. (Nitrogen is the only common element whose mass and valence values are not both even-numbered or both odd-numbered.) PA is present in very low relative concentrations, making its assignment by MS/MS difficult. However, because the molecular ions of PA have significantly lower mass values than those of all other phospholipids detected in negative ion mode, it can be directly identified from the initial negative ion spectrum without MS/MS.

In mass spectral analysis, the same ion is detected with different efficiencies in positive and negative modes, and each phospholipid class will have different efficiencies of detection in a given mode. Therefore, to compare quantitatively the distributions of the phospholipid species, we used PE, which can be detected in both modes, to normalize the positive and negative spectra with respect to each other. In addition, we determined the relative sensitivities of each of the major phospholipid classes using a mixture of known amounts of standards in each of the ion modes as described in Materials and Methods. For the positive ion mode, these values were determined to be 1.00:0.75:0.67 for PC:PE:SM; for the negative ion mode, they are 1.00:1.14:0.46:0.52:0.12 for PI:PG:PS:PA:PE. The low relative efficiency of detection of PE in the negative ion mode may introduce some error in the normalization.

In preliminary experiments, we compared the mass spectra for TLE from RBL-2H3 cells prepared by three different organic solvent-extraction methods: the Folch chloroform:methanol method (*39*), the Bligh and Dyer chloroform:methanol:water method (*40*), and the Ladisch and Gillard diisopropyl ether:butanol:aqueous sodium chloride method (*27*). All three methods gave the same phospholipid components in positive and negative ion spectra, with no more differences in the relative abundance of different components than the observed sample-to-sample variation. We chose the Ladisch and Gillard method as our standard procedure because it allows separation of phospholipids from more hydrophilic gangliosides. Analyses of the phospholipid compositions of TLE, plasma membrane vesicles, and DRM from at least three preparations of each from unstimulated cells are summarized in Table 1 and discussed below. Figure 2

Table 1: Normalized Distributions (%) of Lipids in TLE, PM, and DRM from Unstimulated (u) and Stimulated (s) Cells[a]

	PC (M + H)$^+$				SM (M + H)$^+$				PE (M + H)$^+$				PS (M − H)$^−$				PI (M − H)$^−$				PG (M − H)$^−$				PA (M − H)$^−$			
			DRM				DRM				DRM				DRM				DRM				DRM				DRM	
lipid	TLE	PM	u	s	TLE	PM	u	s	TLE	PM	u	s	TLE	PM	u	s	TLE	PM	u	s	TLE	PM	u	s	TLE	PM	u	s
32:0	0.1	0.8	1.1	0.8																	0.1	.0	.1	0.4	0.3	0.0	0.1	0.0
34:0	0.2	1.4	1.1	0.9					0.0	0.9	1.6	0.9	0.3	0.4	0.4	0.4	0.4	0.5	0.4	0.6	0.3	0.1	0.4	0.4	0.2	0.0	0.1	0.0
36:0	0.3	0.7	0.2	0.9					0.2	1.0	1.8	0.9	0.7	0.8	1.3	1.0	1.0	0.4	1.0	0.7	0.2	0.0	0.5	0.7	0.4	0.2	0.3	0.3
16:0					0.1	2.6	2.5	1.4																				
18:0					0.1	2.2	3.5	3.9																				
24:0					0.0	1.4	3.1	2.0																				
sum *S*	0.5	2.9	2.4	2.6	0.2	6.2	9.1	7.3	0.2	2.0	3.3	1.7	1.0	1.2	1.7	1.4	1.4	0.8	1.5	1.3	0.5	0.1	1.1	1.5	0.9	0.3	0.4	0.3
SD	0.1	0.6	0.5		0.1	1.5	3.3		0.1	0.1	0.2		0.1	0.5	0.5		0.3	0.6	0.3		0.1	0.1	0.6		0.4	0.2	0.1	
32:1	0.3	3.2	1.5	0.0																	0.1	0.0	0.1	0.5	0.1	0.0	0.0	.0
34:1	0.8	8.5	8.5	4.4					0.2	1.5	1.5	0.6	2.4	1.1	2.0	1.3	2.0	0.5	1.1	1.2	1.4	0.1	0.3	0.5	0.5	0.0	0.0	0.0
36:1	0.4	.6	2.4	2.1					0.6	5.3	5.2	1.9	4.4	4.4	7.3	5.0	6.6	1.2	4.6	3.6	0.9	0.2	0.6	0.4	0.7	0.2	0.2	0.1
38:1									0.6	2.2	3.2	1.1	0.3	2.3	0.5	0.5	0.5	0.1	0.5	0.4								
24:1					0.0	2.2	2.8	1.4																				
sum *M*	1.4	15.3	12.4	6.5	0.0	2.2	2.8	1.4	1.3	9.0	9.9	3.7	7.0	7.8	9.7	6.8	9.1	1.8	6.2	5.2	2.4	0.3	1.0	1.4	1.3	0.2	0.2	0.1
SD	0.7	1.8	1.8		0.0	0.8	2.1		0.5	1.0	1.9		1.9	2.8	2.0		1.6	0.7	1.3		0.7	0.2	0.2		0.7	0.2	0.2	
sum *S* + *M*	2.0	18.3	14.8	9.1	0.2	8.4	11.9	8.7	1.5	10.9	13.3	5.4	8.0	8.9	11.5	8.2	10.4	2.7	7.7	6.5	2.9	0.4	2.1	2.9	2.2	0.4	0.7	0.3
SD	0.7	1.9	1.8		0.1	1.7	3.9		0.6	1.0	1.9		1.9	2.9	2.0		1.7	0.9	1.3		0.7	0.2	0.6		0.8	0.2	0.2	
32:2	0.1	0.4	0.2	0.3																					0.1	0.0	0.1	0.0
34:2	0.3	.1	0.9	0.7									0.3	0.2	0.2	0.0	0.3	0.2	0.2	0.2					0.1	0.0	0.1	0.0
34:3	0.8	0.5	0.5	1.7																								
34:4	2.8	1.8	0.9	2.1																								
34:5	0.3	1.0	0.2	0.3																								
36:2	0.6	4.5	1.9	1.3					0.2	1.0	0.7	0.5	1.8	1.2	1.9	1.0	3.4	0.7	1.3	0.9	1.3	0.0	0.3	0.1				
36:3	1.9	1.3	1.2	2.1					0.6	0.4	0.5	1.3	0.2	0.2	0.1	0.0												
36:4	10.7	5.8	4.0	7.4					1.2	0.6	0.4	1.1	0.2	0.1	0.1	0.9												
36:5	1.7	1.4	0.2	1.2																								
38:2		0.4							0.6	1.2	1.1	0.6	0.5	1.3	0.6	0.5	1.5	0.4	1.4	0.9								
38:3	0.7	0.6	0.0	0.0					1.4	0.8	0.7	2.0	0.4	0.6	0.8	0.8	1.9	0.7	1.2	1.0								
38:4	4.0	2.5	1.3	4.1					4.5	2.6	1.8	4.2	0.8	1.7	0.9	1.0	1.9	0.8	1.2	1.3	0.1	0.1	0.1	0.0				
38:5	6.5	3.6	1.4	3.3					1.0	0.7	0.5	1.2	0.4	0.5	0.3	0.9	0.6	0.1	0.2	0.3	0.1	0.0	0.2	0.2				
38:6	0.4	0.6	0.0	0.6																	0.2	0.0	0.1	0.2				
40:3		0.3							0.9	0.6	0.5	0.4																
40:4	0.2	0.2	0.1	0.0					2.0	1.1	1.1	2.5					0.6	0.3	0.4	0.3	0.2	0.0	0.2	0.2				
40:5	0.6	0.2	0.3	0.7					1.5	1.1	0.7	1.6	1.9				1.7	0.7	1.2	1.2	0.2	0.1	0.2	0.3				
40:6	0.3	0.5	0.3	0.8					0.4	0.7			1.0				1.7	0.8	1.2	1.1	0.6	0.0	0.4	0.4				
40:7																					1.8	0.0	0.5	0.2				
42:5																					0.2	0.0	0.2	0.1				
42:6																					0.7	0.1	0.5	0.3				
42:7																					0.2	0.0	0.1	0.1				
18:2					0.2	0.3	0.1	0.0																				
20:2					0.0	0.4	0.8	1.8																				
sum *P*	31.8	27.5	13.3	26.5	0.2	0.7	0.8	1.8	14.2	10.7	7.9	15.5	7.4	5.8	5.0	5.0	13.6	4.7	8.3	7.3	5.5	0.5	2.8	2.1	0.1	0.0	0.1	0.0
SD	2.7	2.2	.3		0.2	0.2	0.3		1.2	0.7	0.7		0.6	2.4	0.9		1.9	0.9	1.0		1.5	0.2	.8		0.5	0.2	0.2	
total	33.7	45.8	28.1	36.3	0.4	9.1	12.8	10.5	15.7	21.6	21.2	20.9	15.4	14.7	16.5	13.3	24.0	7.4	16.0	13.8	8.4	0.9	4.9	5.0	2.3	0.4	0.7	0.3
SD	2.8	2.9	2.3		0.2	1.7	3.2		1.3	1.2	2.0		2.0	3.7	2.2		2.5	1.3	1.6		1.5	0.2	0.6		0.5	0.2	0.2	

[a] For TLE, compositions are the average of 4 datasets; for plasma membranes and DRM from unstimulated cells, 3 datasets for each are averaged; compositions for DRM from stimulated cells are from 1 representative sample. For clarity, standard deviations are shown only for the sums within each saturation group. *S* is saturated; *M* is monounsaturated, and *P* is polyunsaturated.

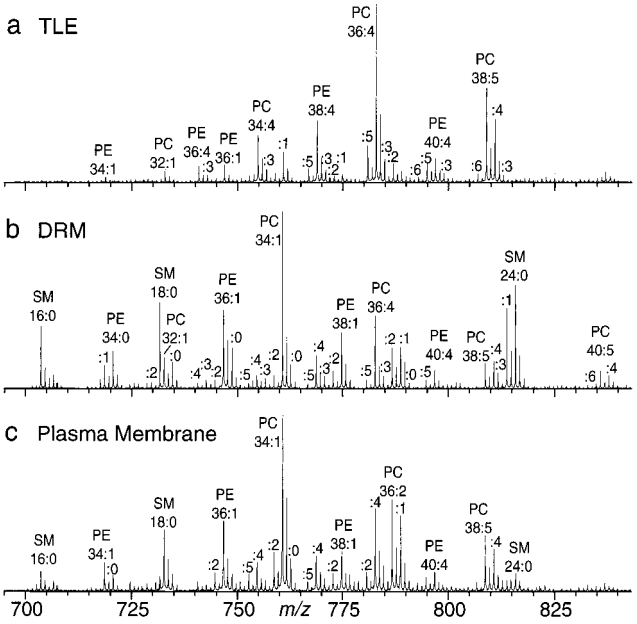

FIGURE 2: Representative positive ion spectra of TLE (a), DRM vesicles (b), and plasma membrane vesicles (c), extracted and analyzed under identical conditions. Labels identify the most abundant PL species and show the total number of carbons and double bonds in the acyl chains. Note that each species produces a $^{12}C_n$ peak and a smaller $^{13}C_1{}^{12}C_{n-1}$ peak, as shown in Figure 1.

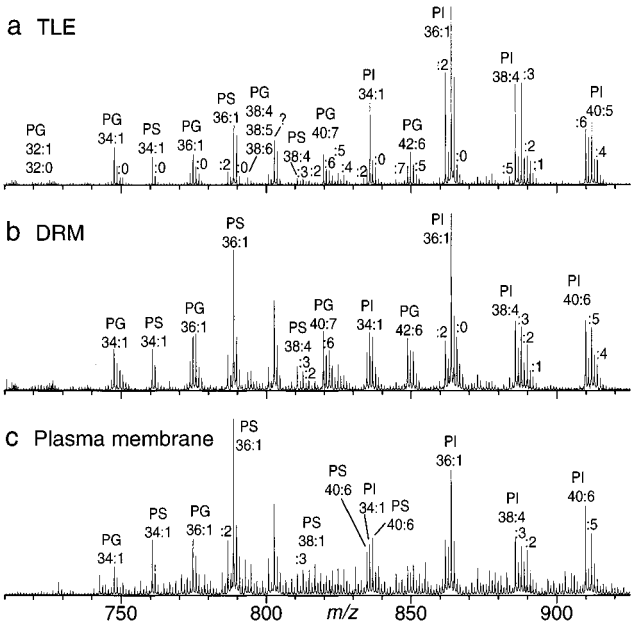

FIGURE 3: Representative negative ion spectrum of TLE (a), DRM vesicles (b), and plasma membrane vesicles (c). Labels are as described in the legend to Figure 2. "?" indicates unidentified species.

shows a representative positive ion spectrum of TLE (top) and compares it to a spectrum of DRM vesicles (middle) and a spectrum of plasma membrane vesicles (bottom); all three samples were extracted by the same method and analyzed under identical conditions. Multiple PE and PC species with different acyl chain lengths and different numbers of double bonds are revealed, and molecules with 3, 4, or 5 double bonds are the most abundant in the TLE spectrum. The DRM spectrum shown in the middle panel contains nearly all the same phospholipid species identified in the TLE spectrum, but with distinctive distributions. For the major glycerophospholipids detected (PC, PE) over 60% of these in DRMs are molecules with two saturated or one saturated and one monounsaturated acyl chain, whereas this group represents less than 10% of PC and PE in TLE. Although barely detectable in the TLE spectrum, SM species of several different acyl chain lengths are major components in DRM. The largest abundance of SM are those containing one or no double bonds, similar to the predominance of glycerophospholipids PC and PE containing saturated and/or pauci-unsaturated acyl chains in the DRM composition. The positive ion spectrum of the plasma membrane vesicle preparation (Figure 2, bottom) appears similar to that of the DRM, but quantitative analyses reveal significant differences in the headgroup distributions and the percentage of polyunsaturated phospholipids as described below.

Figure 3 shows representative negative ion spectra for TLE, DRM, and plasma membranes, in which PI, PG, PS, and PA species are identified. In these cells, PI is the most abundant negatively charged phospholipid, with a wide distribution of acyl chain lengths and degrees of saturation. However, we did not detect polyphosphoinositol lipids which are expected to be minor components compared with PI (*41*). (It is possible that these more polar phospholipids are selectively depleted from the organic phase during the extraction procedure.) Differences in the relative abundance of phospholipid species detected in negative ion mode between TLE and DRM or plasma membranes are not as apparent by visual inspection as these differences in positive ion spectra, in part because negative phospholipids with saturated or monounsaturated acyl chains are more abundant in TLE than their zwitterionic counterparts. Nevertheless, quantitative analysis reveals significant differences for negatively charged phospholipids among the different preparations as described below.

Table 1 summarizes the quantitative analyses of the phospholipids from each of four different types of preparation, including one of two consistent data sets for DRM from stimulated cells. The most striking feature of total phospholipid compositions in the last line of Table 1 is that the SM in unstimulated DRM is enriched ~30-fold as compared to SM in TLE. Plasma membrane vesicles are also highly enriched in SM relative to TLE (~20-fold), and these results are qualitatively consistent with previous lipid analyses of DRM (*5*) and plasma membranes (*42*). Other notable differences in the total lipid compositions are a substantial enrichment in PC and corresponding depletions of PI and PG in plasma membrane vesicles compared with either TLE or DRM. The reasons for these differences are not known, but they indicate that DRM lipids are a distinct subset of the plasma membranes from which they are primarily derived (*43*). Comparison of the relative contributions of polyunsaturated phospholipids to saturated and monounsaturated phospholipids reveals a particularly interesting trend: as tabulated for individual headgroups in Table 1 and summarized in Figure 4, over 60% of the phospholipids in unstimulated DRM contain 1 or no double bond, whereas less than 30% have these characteristics in TLE. Plasma membrane vesicles are intermediate in this comparison, with 50% of the phospholipids containing 1 or no double bond, and 50% with 2 or more double bonds (i.e., polyunsaturated;

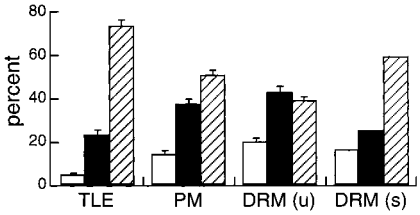

FIGURE 4: Percent of total phospholipids in each preparation that contain no double bonds in acyl chain (open bars), 1 double bond in acyl chains (filled bars), or more than 1 double bond in acyl chains (polyunsaturated; hatched bars). Error bars show the rms standard deviations from the sums of the data in Table 1.

hatched bars, Figure 4). Liquid-ordered structure is highly favored for model membranes with high cholesterol and saturated and monounsaturated phospholipids (*5*); thus, our results are consistent with expectations of a high degree of liquid order in unstimulated DRM (see Discussion).

We also investigated whether the phospholipid composition of DRM vesicles isolated from stimulated cells showed differences from those isolated from unstimulated cells. For these experiments, biotinylated IgE bound to FcϵRI on intact cells was cross-linked with streptavidin for 5 min at 37 °C prior to cell lysis and isolation of DRM vesicles. Under these conditions, 50−60% of IgE−FcϵRI co-isolate with DRM vesicles, but little or no additional changes in protein composition of these vesicles are detected (*11*) (K. Field, D. Holowka, B. Baird, unpublished results). As represented by the data from one experiment in Table 1 and Figure 4, the mass spectra from two independent experiments show a reproducible increase in the abundance of polyunsaturated phospholipids and a corresponding decrease in the abundance of saturated and monounsaturated species for the DRM from stimulated cells compared to those from unstimulated cells. The large increase in percent polyunsaturated phospholipids observed (12−22% in two experiments) is surprising, since it results in a greater percent contribution of these polyunsaturated lipids to stimulated DRM than found in unstimulated plasma membrane vesicles (Figure 4). This suggests that stimulation for 5 min at 37 °C causes substantial lipid remodeling, possibly including the recruitment of intracellular membranes to the plasma membrane. Further study will be necessary to investigate this possibility.

DISCUSSION

It has been evident for some time that the lipid composition of membranes from different organelles in eukaryotic cells can differ substantially. For example, the plasma membrane is known to be more highly enriched in cholesterol and SM than most intracellular membranes (*44*). Furthermore, transbilayer asymmetry of phospholipids is well-documented, particularly in erythrocyte plasma membranes for which lipid analyses are not complicated by contamination from intracellular organelles (*44*). The physiological significance of these various types of lipid heterogeneities has, for the most part, remained poorly understood. This is partially due in part to the enormous number of different cellular phospholipid species and to previous limitations in sensitivity and resolution of analytical methods.

Recent studies by Brown and colleagues suggest that SM and cholesterol facilitate lateral separations of proteins and lipids in plasma membranes with important physiological consequences (*5, 43*). They showed that model membrane bilayers with a relatively high ratio of cholesterol to phospholipid have a L_o structure, which is critical for the detergent-resistant properties of a subset of plasma membrane proteins and lipids (*4, 6*). Furthermore, these studies provide evidence that detergent-resistant membrane domains rich in cholesterol and SM can co-exist with the less ordered, liquid-crystalline regions of the model membranes. These data support the view that L_o and liquid-crystalline regions also can co-exist in the plasma membrane of functioning cells and that the DRM vesicles isolated from Triton X-100 lysates of eukaryotic cells represent the same components that form L_o regions in the plasma membrane. Our recent studies indicate that interactions between cross-linked FcϵRI and Lyn that lead to mast cell activation depend on mutual interactions of these proteins with DRM (*11, 15, 45*). Furthermore, cholesterol plays a critical role in these interactions (*16*), and this provides strong evidence for a functional role for DRM on cells.

Our present results are consistent with those of Brown and Rose (*3*), who showed with sucrose gradient and TLC analyses that virtually all of the cellular SM as well as glycosphingolipids were recovered in DRM vesicles derived from MDCK cells; much smaller percentages of total cellular glycerophospholipids were present in these vesicles. Mescher and Apgar (*46*) characterized a similar Triton X-100-resistant fraction from highly purified leukocyte plasma membranes, and they found that all of the SM and nearly 40% of all plasma membrane phospholipids were recovered with their DRM components suggesting that a substantial percentage of the plasma membrane is liquid-ordered. Studies with model membranes predict that DRM vesicles should be enriched in phospholipids with saturated and monounsaturated acyl chains for optimal formation of liquid-ordered structure (*5*). Our mass spectrometry results demonstrate the predominance of phospholipids with these characteristics in unstimulated DRM from unstimulated cells (62%; Figure 4) and indicate that these lipids are also abundant in plasma membrane vesicles (50%), consistent with the hypothesis that DRM are liquid-ordered and represent a substantial fraction of the plasma membrane. Recent electron spin resonance measurements on DRM vesicles isolated from RBL-2H3 cells with the same procedure support this view (*47*).

Negatively charged phospholipids isolated with DRM (PS, PI, PG, and PA) show preference for molecules with 1 or no unsaturated acyl chain (58%), similar to these species for the zwitterionic phospholipids (PC, SM, and PE) in DRM (65%). PE, PS, and PI are likely to be enriched in the inner leaflet of the plasma membrane, whereas PC and SM are enriched in the outer leaflet (*44*), so our results are consistent with substantial amounts of liquid order in each, assuming that cholesterol is equally distributed in both leaflets. It is possible that certain negatively charged phospholipids may be enriched in DRM vesicles relative to the entire plasma membrane because of headgroup interactions. This possibility is particularly interesting for the polyphosphatidylinositols that serve as specific docking sites and substrates for key signaling proteins and enzymes (*48*). A recent study indicates that polyphosphatidylinositol 4,5-bisphosphate is more highly enriched than PI in DRM (*49*).

Our present results provide the first detailed view of the phospholipid composition in isolated DRM, particularly with

respect to acyl chain composition, and these results support the hypothesis of Brown and London for the L_o structural basis of DRM stability in the presence of micellar Triton X-100 (*5*). It is important to note that our analysis was carried out on DRM vesicles isolated after lysis in concentrations of Triton X-100 (0.04−0.05% v/v) that are lower than those used in previous analyses of DRM lipid composition (typically 0.2−1.0% v/v). Our choice of detergent concentration is based on the requirement for this lower amount of detergent to preserve interactions between aggregated FcεRI and DRM vesicles (*11*, *15*) and our intent to investigate whether FcεRI association could alter the lipid composition. We previously determined that there is little or no difference in the protein composition of DRM vesicles isolated after cell lysis with 0.05% vs 0.2% Triton X-100 (*11*) and that other transmembrane receptors do not associate with DRM vesicles, even at this lower detergent concentration (*45*). The dependence on receptor aggregation of FcεRI association with DRM vesicles highlights the selectivity of this interaction. We attempted to compare the lipid composition of DRM isolated from cells lysed in 0.2% Triton X-100, but high residual concentrations of Triton X-100 in these preparations overwhelmed the sensitive mass spectrometric measurements.

Our analysis of the lipid composition of DRM vesicles isolated from cells that were activated by IgE−FcεRI cross-linking is limited, but some small differences in headgroup distributions compared to DRM vesicles from unstimulated cells are apparent, and more substantial differences in the percentage of polyunsaturated glycerophospholipids are clear (Table 1 and Figure 4). This may be related to the aggregation-induced association of FcεRI with these vesicles, but the percent increase in DRM polyunsaturated phospholipids due to stimulation that is observed is probably too great to be accounted for by the recruitment of FcεRI annular lipids.[2] It is interesting that more than 50% of the phospholipids from DRMs isolated after stimulation are polyunsaturated, since these would be expected to promote disorder and solubility by TX-100. It is possible that other factors, such as an increase in plasma membrane cholesterol due to stimulation, can compensate for the increase in polyunsaturated phospholipids. The conditions for stimulation in the present study (5 min, 37 °C) were chosen to maximize receptor association with isolated DRM, and potential changes in DRM phospholipids caused by stimulated lipid metabolism or stimulated recruitment of intracellular membrane may contribute to the observed changes. Longer periods of stimulation will be investigated in future experiments, since these might cause even more dramatic changes in DRM lipid composition. For example, stimulation by epidermal growth factor resulted in selective hydrolysis of polyphosphatidylinositols in DRM from A431 cells (*51*).

In summary, our results provide a detailed view and new insight into the structural composition of DRM, and they demonstrate the power of FTMS analysis of phospholipids from complex biological membranes. We anticipate that refinements in methods of isolation will allow similar analyses of glycolipid composition, also likely to be important to the structure and function of specialized domains within plasma membranes of eukaryotic cells.

[2] Assuming that DRM contain 30% of the plasma membrane lipids and that plasma membranes comprise 5% of the total RBL-2H3 membranes, then the association of 50% of FcεRI due to cross-linking (*11*) results in the recruitment of $\sim 10^3$ polyunsaturated phospholipid species per receptor. Annular lipids are likely to be ≪100 per receptor (*50*).

REFERENCES

1. Edidin, M. (1997) *Curr. Opin. Struct. Biol. 7*, 528−532.
2. Hooper, N. M., and Turner, A. J. (1988) *Biochem. J. 250*, 865−869.
3. Brown, D. A., and Rose, J. K. (1992) *Cell 68*, 533−544.
4. Schroeder, R., London, E., and Brown, D. (1994) *Proc. Natl. Acad. Sci. U.S.A. 91*, 12130−12134.
5. Brown, D. A., and London, E. (1998) *J. Membr. Biol. 164*, 103−114.
6. Ahmed, S. N., Brown, D. A., and London, E. (1997) *Biochemistry 36*, 10944−10953.
7. Recktenwald, D. J., and McConnell, H. M. (1981) *Biochemistry 20*, 4505−4510.
8. Ipsen, J. H., Mouritsen, O. G., and Bloom, M. (1990) *Biophys. J. 57*, 405−412.
9. Sankaram, M. B., and Thompson, T. E. (1991) *Proc. Natl. Acad. Sci. U.S.A. 88*, 8686−8690.
10. Silvius, J. R., del Giudice, D., and Lafleur, M. (1996) *Biochemistry 35*, 15198−15208.
11. Field, K. A., Holowka, D., and Baird, B. (1997) *J. Biol. Chem. 272*, 4276−4280.
12. Sheets, E. D., Holowka, D., and Baird, B. (1999) *Curr. Opin. Chem. Biol. 3*, 95−99.
13. Shenoy-Scaria, A. M., Dietzen, D. J., Kwong, J., Link, D. C., and Lublin, D. M. (1994) *J. Cell Biol. 126*, 353−363.
14. van't Hof, W., and Resh, M. D. (1997) *J. Cell Biol. 136*, 1023−1035.
15. Field, K. A., Holowka, D., and Baird, B. (1995) *Proc. Natl. Acad. Sci. U.S.A. 92*, 9201−9205.
16. Sheets, E. D., Holowka, D., and Baird, B. (1999) *J. Cell Biol. 145*, 877−887.
17. Han, X., and Gross, R. W. (1994) *Proc. Natl. Acad. Sci. U.S.A. 91*, 10635−10639.
18. Han, X. L., and Gross, R. W. (1995) *J. Am. Soc. Mass Spectrom. 6*, 1202−1210.
19. Brugger, B., Erben, G., Sandhoff, R., Wieland, F. T., and Lehmann, W. D. (1997) *Proc. Natl. Acad. Sci. U.S.A. 94*, 2339−2344.
20. Metzger, K., Rehberger, P. A., Erben, G., and Lehmann, W. D. (1995) *Anal. Chem. 67*, 4178−4183.
21. Han, X., Gubitosi-Klug, R. A., Collins, B. J., and Gross, R. W. (1996) *Biochemistry 35*, 5822−5832.
22. Ramanadham, S., Hsu, F. F., Bohrer, A., Nowatzke, W., Ma, Z., and Turk, J. (1998) *Biochemistry 37*, 4553−4567.
23. Jensen, N. J., and Gross, M. L. (1988) *Mass Spectrom. Rev. 7*, 41−69.
24. Fenn, J. B., Mann, M., Meng, C. K., Wong, S. F., and Whitehouse, C. M. (1989) *Science 246*, 64−71.
25. Marto, J. A., White, F. M., Seldomridge, S., and Marshall, A. G. (1995) *Anal. Chem. 67*, 3979−3984.
26. Pierini, L., Harris, N. T., Holowka, D., and Baird, B. (1997) *Biochemistry 36*, 7447−7456.
27. Ladisch, S., and Gillard, B. (1985) *Anal. Biochem. 146*, 220−231.
28. Holowka, D., and Baird, B. (1984) *J. Biol. Chem. 259*, 3720−3728.
29. Holowka, D., and Baird, B. (1983) *Biochemistry 22*, 3466−3474.
30. Menon, A. K., Holowka, D., Webb, W. W., and Baird, B. (1986) *J. Cell Biol. 102*, 541−550.
31. Wilm, M. S., and Mann, M. (1994) *Int. J. Mass Spectrom. Ion Processes 136*, 167−180.
32. Wilm, M., and Mann, M. (1996) *Anal. Chem. 68*, 1−8.
33. Chang, E. Y., Zheng, Y., Holowka, D., and Baird, B. (1995) *Biochemistry 34*, 4376−4384.
34. Beu, S. C., Senko, M. W., Quinn, J. P., Wampler, F. M., and McLafferty, F. W. (1993) *J. Am. Soc. Mass Spectrom. 4*, 557−565.

35. Marshall, A. G., Wang, T. C. L., and Ricca, T. L. (1985) *J. Am. Chem. Soc. 107*, 7893−7897.
36. Loo, J. A., Udseth, H. R., and Smith, R. D. (1988) *Rapid Commun. Mass Spectrom. 2*, 207−210.
37. Gauthier, J. W., Trautman, T. R., and Jacobson, D. B. (1991) *Anal. Chim. Acta 246*, 211−225.
38. Senko, M. W., Speir, J. P., and McLafferty, F. W. (1994) *Anal. Chem. 66*, 2801−2808.
39. Folch, J., Lees, M., and Stanley, G. H. S. (1957) *J. Biol. Chem. 226*, 497−509.
40. Bligh, E. G., and Dyer, W. J. (1959) *Can. J. Biochem. Physiol. 37*, 911−917.
41. Lo, T. N., Saul, W., and Beaven, M. A. (1987) *J. Biol. Chem. 262*, 4141−4145.
42. Scott, R. E., Perkins, R. G., Zschunke, M. A., Hoerl, B. J., and Maercklein, P. B. (1979) *J. Cell Sci. 35*, 229−243.
43. Brown, D. A., and London, E. (1998) *Annu. Rev. Cell Biol. 14*, 111−136.
44. Devaux, P. F. (1991) *Biochemistry 30*, 1163−1173.
45. Field, K. A., Holowka, D., and Baird, B. (1999) *J. Biol. Chem. 274*, 1753−1758.
46. Mescher, M. F., and Apgar, J. R. (1985) *Adv. Exp. Med. Biol. 184*, 387−400.
47. Ge, M., Field, K. A., Aneja, R., Holowka, D., Baird, B., and Freed, J. (1999) *Biophys. J.* (in press).
48. Toker, A., and Cantley, L. C. (1997) *Nature 387*, 673−676.
49. Liu, Y., Casey, L., and Pike, L. J. (1998) *Biochem. Biophys. Res. Commun. 245*, 684−690.
50. Thomas, J. L., Holowka, D., Baird, B., and Webb, W. W. (1994) *J. Cell Biol. 125*, 795−802.
51. Pike, L. J., and Miller, J. M. (1998) *J. Biol. Chem. 273*, 22298−22304.

BI9828324